## Title

THE TRANSIENT, STEADY STATE AND STABILITY BEHAVIOR OF A THERMOSYPHON WITH THROUGHFLOW



## Authors

Mertol, A.
Greif, R.
Zvirin, Y.

## Publication Date

1981-04-01

Lawrence Berkeley Laboratory
UNIVERSITY OF CALIFORNIA

ENERGY & ENVIRONMENT
DIVISION

Submitted to the International Journal of Heat and Mass Transfer

# THE TRANSIENT, STEADY STATE AND STABILITY BEHAVIOR OF A THERMOSYPHON WITH THROUGHFLOW

A. Mertol, R. Greif, and Y. Zvirin

April 1981



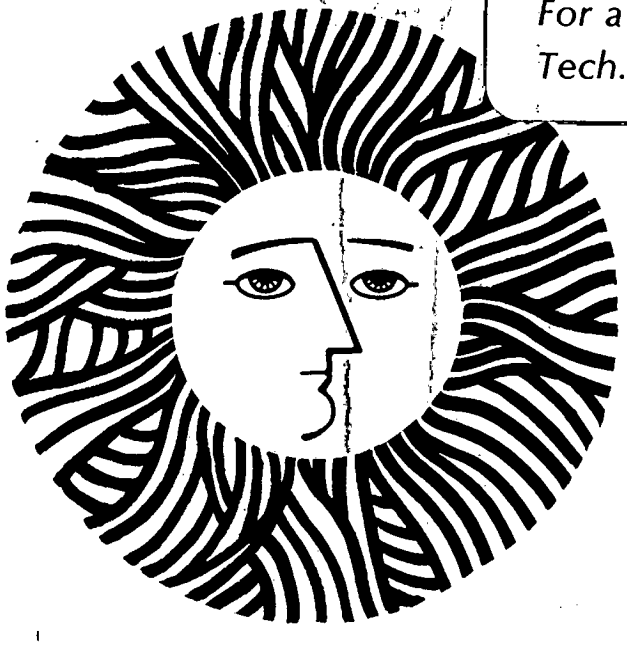

Prepared for the U.S. Department of Energy under Contract W-7405-ENG-48

## DISCLAIMER

# "The Transient, Steady State and Stability Behavior of a Thermosyphon with Throughflow"*

by

A. Mertol and R. Greif

Passive Solar Analysis and Design Group,
Lawrence Berkeley Laboratory and Department of Mechanical Engineering
University of California, Berkeley, CA 94720

Y. Zvirin
Faculty of Mechanical Engineering, Technion
Israel Institute of Technology
Haifa, Israel

On leave, Electric Power Research Institute
Palo Alto, CA 94303

## Abstract

A study has been made of the flow, heat transfer and stability of a natural convection loop when there is an addition and withdrawal of fluid. The loop is a toroid that is oriented in a vertical plane and is heated over the lower half and cooled, by maintaining a constant wall temperature, on the upper half. The results include stable, as well as unstable configurations and also reveal multiple solutions.

---

*This work was supported by the Research and Development Branch, Passive and Hybrid Division, of the Office of Solar Applications for Buildings, U.S. Department of Energy, under Contract No. W-7405-ENG-48.

## NOMENCLATURE

| | | |
|---|---|---|
| $A$ | = | cross-sectional area of the toroid |
| $c$ | = | specific heat |
| $D$ | = | dimensionless parameter, Eq. (11) |
| $F$ | = | heat flux |
| $f$ | = | friction coefficient |
| $g$ | = | acceleration of gravity |
| $h$ | = | heat transfer coefficient |
| $M$ | = | total number of grids |
| $p$ | = | pressure |
| $q$ | = | volumetric flow rate of the circulating fluid in the system |
| $R$ | = | radius of the circular loop, Fig. 1 |
| $Re$ | = | Reynolds number |
| $r$ | = | radius of the toroid, Fig. 1 |
| $T$ | = | temperature |
| $t$ | = | time |
| $V$ | = | characteristic velocity, Eq. (8) |
| $v$ | = | velocity of the circulating fluid |
| $w$ | = | dimensionless volumetric flow rate or velocity, Eq. (7) |

### Greek Symbols

| | | |
|---|---|---|
| $\beta$ | = | thermal expansion coefficient |
| $\Gamma$ | = | dimensionless parameter, Eq. (11) |
| $\eta$ | = | efficiency, Eqs. (15), (16) and (17) |
| $\theta$ | = | space coordinate, Fig. 1 |
| $\theta_p$ | = | thermal penetration depth |

$\kappa$ = dimensionless volumetric throughflow rate, Eq. (7)

$\kappa^*$ = volumetric throughflow rate

$\mu$ = absolute viscosity

$\rho$ = density

$\tau$ = dimensionless time, Eq. (7)

$\tau_w$ = wall shear stress

$\phi$ = dimensionless temperature, Eq. (7)

Subscripts

0 = location at $\theta = 0$

ch = characteristic

i = initial value, space step in the finite difference equations

in = inlet

l = lower portion of the loop

M = location at $\theta = 2\pi$

n = time step in the finite difference equations

ss = steady-state

u = upper portion of the loop

w = wall

## INTRODUCTION

This paper is concerned with the transient and steady state behavior and stability of natural convection loops; i.e. thermosyphons, when there is an addition and withdrawal of fluid (throughflow). Increasing interest in this area has occurred in respect to applications in solar energy, nuclear reactor cooling and geothermal systems. Most studies have been carried out for closed loops, that is, without a throughflow. This includes the early stability studies of the steady state motion by Keller [1] and Welander [2] for the simple geometry consisting of a point heat source and sink with two vertical branches. Creveling, et al [3] and Damerell and Schoenhals [4] considered a toroidal loop and showed, experimentally and theoretically, the presence and importance of instabilities. Zvirin, Shitzer and Grossman [5] and Zvirin et al [6] studied the stability characteristics of the thermosyphonic solar water heater and showed that this system can become unstable at high energy utilizations. Mertol, Place, Webster and Greif [7,8] studied the transient daytime and nighttime performance of a thermosyphon solar water heater with a heat-exchanger in the storage tank and found, analytically, that the flow reverses during the night but the magnitude of the reverse flow is reduced when high viscosity fluids, such as propylene glycol are used. It was also observed that low viscosity fluids have strong oscillations during the night. A study of the transient behavior and stability of the toroidal loop was carried out by Greif, Zvirin and Mertol [9] and Mertol [10]. Other studies by Japikse [11], Zvirin et al [12,13] and Ong [14,15] should also be noted.

The references cited above refer to closed loops and much less information is available on open thermosyphons. Torrance [16] studied

the steady flow and heat transfer in an open geothermal system where the inlet and outlet are at a boundary of the medium. Zvirin [17,18] studied the effects of a throughflow on the loop with two vertical branches with a point heat source and sink.

The present work analyzes the steady state, transient and stability behavior of an open toroidal loop. The loop is oriented in a vertical plane which is heated over the lower half and cooled by maintaining a constant wall temperature on the upper half (cf. Fig. 1). The conservation equations are averaged over the cross-section and an analytical solution is derived for the steady state condition. A numerical method is used to obtain the transient flow and heat transfer by solving simultaneously the momentum and energy equations. The numerical method is also used to evaluate the stability characteristics of the system and small amplitude instabilities associated with oscillatory motion in thermosyphons have been shown to be present. In addition, the steady state motion reveals another type of instability associated with multiple solutions (double or triple) for certain ranges of the system and throughflow parameters.

## ANALYSIS

The analysis which follows predicts the transient and steady state volumetric flow rate and temperature profiles in an open toroidal thermosyphon with throughflow. The loop is heated continuously by a constant heat flux F over the bottom half and is cooled continuously over the top half by maintaining a constant wall temperature at $T_w$ (cf. Fig. 1). A constant volumetric throughflow rate, $\kappa^*$, is maintained with the inlet at the entrance to the heated region, $\theta = \pi$, and the outlet at the exit from the heated region, $\theta = 0$ or $2\pi$. Perfect mixing is assumed to occur at the inlet, between $\theta = \pi^-$ and $\pi^+$.

The conservation equations; continuity, momentum and energy, are averaged over the cross-section [3, 9] so that the control volume is of diameter 2r and length $Rd\theta$ (cf. Fig. 1). The flow is assumed to be laminar and the fluid properties are taken as constant except in the buoyancy term in which the Boussinesq approximation is used. Viscous heating, axial conduction and curvature effects are neglected.

From the equation of continuity for one-dimensional incompressible flow, we have that the velocity and the volumetric flow rate are functions of time only. In the upper region this is given by

$$q_u(t) = \pi r^2 v_u(t) \tag{1a}$$

and in the lower region by

$$q_\ell(t) = q_u(t) + \kappa^* = \pi r^2 v_\ell(t) = \pi r^2 [v_u(t) + \frac{\kappa^*}{\pi r^2}] \tag{1b}$$

The momentum equation in the $\theta$ direction for these regions is:

$$\rho \frac{dv_{u,\ell}}{dt} = -\frac{1}{R}\frac{dp}{d\theta} - \rho g \cos\theta - \frac{2\tau_w}{r} \tag{2}$$

where $v_u$ and $v_\ell$ are used in the upper and lower regions, respectively. Multiplying Eq. (2) by the cross-sectional area, $A = \pi r^2$, using the relation $\rho = \rho_w [1-\beta(T-T_w)]$ in the body force term, and integrating around the loop yields the following equations for the upper and lower regions, respectively:

$$\rho_w \frac{dq}{dt} = -\frac{r^2}{R}[p(\pi^-,t)-p(o,t)] + \rho_w g r^2 \beta \int_o^{\pi^-}(T-T_w)\cos\theta d\theta - \tau_{w,u} 2\pi r, \quad 0 < \theta < \pi \tag{3a}$$

and

$$\rho_w \frac{d}{dt}(q + \kappa^*) = -\frac{r^2}{R}[p(2\pi,t) - p(\pi^+,t)] + \tag{3b}$$

$$\rho_w g r^2 \beta \int_{\pi^+}^{2\pi}(T-T_w)\cos\theta d\theta - \tau_{w,\ell} 2\pi r, \quad \pi < \theta < 2\pi$$

where $q \equiv q_u$. Adding Eqs. (3a) and (3b) and using continuity of the pressure:

$$p(\pi^-,t) = p(\pi^+,t) \quad , \quad p(o,t) = p(2\pi,t) \tag{4}$$

yields

$$\rho_w \frac{d}{dt}(2q + \kappa^*) = \rho_w g r^2 \beta \int_0^{2\pi} (T-T_w)\cos\theta d\theta - 2\pi r(\tau_{w,u} + \tau_{w,\ell}) \tag{5}$$

To solve for the volumetric flow rate from Eq. (5), it is necessary to obtain the temperature variation, $T(\theta,t)$. The energy equations for the heated lower and cooled upper regions are given by:

$$\rho_w c \left[\frac{\partial T}{\partial t} + \frac{q}{\pi r^2 R} \frac{\partial T}{\partial \theta}\right] = -\frac{2h}{r}(T-T_w), \qquad 0 < \theta < \pi \tag{6a}$$

and

$$\rho_w c \left[\frac{\partial T}{\partial t} + \frac{(q + \kappa^*)}{\pi r^2 R} \frac{\partial T}{\partial \theta}\right] = \frac{2F}{r}, \qquad \pi < \theta < 2\pi \tag{6b}$$

Eqs. (5) and (6) must be solved simultaneously to obtain the volumetric flow rate and the temperature profiles.

The governing equations are made dimensionless by defining the following relations:

$$\phi = \frac{T-T_w}{F/h}, \quad w = \frac{q}{q_{ch}}, \quad \kappa = \frac{\kappa^*}{q_{ch}}, \quad \tau = \frac{t}{2\pi R/V} \tag{7}$$

where $q_{ch}$ is the characteristic volumetric flow rate defined as the product of the characteristic velocity, V, and the cross-sectional area, A, (cf. Creveling et al. [3]).

$$q_{ch} = AV = \pi r^2 V = \pi r^2 \left(\frac{q\beta RrF}{2\pi c\mu}\right)^{1/2} \tag{8}$$

The wall shear stresses in Eq. (5) are expressed as $\tau_{w,u} = \frac{1}{2} f_u \rho_w \frac{q^2}{A^2}$ and $\tau_{w,\ell} = \frac{1}{2} f_\ell \rho_w \frac{(q + \kappa^*)^2}{A^2}$, for the upper and lower portions of the loop, respectively, where the friction coefficients for laminar flow are given by $f_{u,\ell} = 16/Re_{u,\ell}$ with $Re_u = 2\rho_w q/\mu\pi r$ and $Re_\ell = 2\rho_w(q + \kappa^*)/\mu\pi r$.

The dimensionless forms of Eqs. (5) and (6) then become

$$\frac{d}{d\tau}\left(w + \frac{\kappa}{2}\right) + \Gamma\left(w + \frac{\kappa}{2}\right) = \frac{\pi}{4}\frac{\Gamma}{D}\int_0^{2\pi} \phi \cos\theta d\theta \tag{9}$$

$$\frac{\partial\phi}{\partial\tau} + 2\pi w \frac{\partial\phi}{\partial\theta} = -2D\phi \quad , \quad 0 < \theta < \pi \tag{10a}$$

and

$$\frac{\partial\phi}{\partial\tau} + 2\pi (w + \kappa) \frac{\partial\phi}{\partial\theta} = 2D \quad , \quad \pi < \theta < 2\pi \tag{10b}$$

where the dimensionless system parameters D and $\Gamma$ are defined by

$$D = \frac{2\pi Rh}{\rho_w crV} \quad \text{and} \quad \Gamma = \frac{16\pi\mu R}{\rho_w r^2 V} \tag{11}$$

Steady-State Solutions

The steady-state temperature profile is obtained by solving Eqs. (10) with $\partial\phi/\partial\tau = 0$ subject to the conditions of temperature continuity at the outlet:

$$\phi_{ss}(0) = \phi_{ss}(2\pi) \tag{12a}$$

and an energy balance at the inlet:

$$\phi_{ss}(\pi^+) = \frac{w_{ss}}{w_{ss} + \kappa}\ \phi_{ss}(\pi^-) + \frac{\kappa}{w_{ss} + \kappa}\ \phi_{in} \tag{12b}$$

The results are

$$\phi(\theta) = \phi_{ss} = \begin{cases} \left[\dfrac{D + \kappa\phi_{in}}{\kappa + w_{ss}\left(1-e^{-D/w_{ss}}\right)}\right] e^{-\frac{D}{w_{ss}}\frac{\theta}{\pi}}, & 0 < \theta < \pi \\ \dfrac{D}{(w_{ss} + \kappa)}\left[\dfrac{\theta}{\pi} + \dfrac{w_{ss}\left(2e^{-D/w_{ss}} - 1\right) + \frac{\kappa}{D}\phi_{in}(w_{ss} + \kappa) - \kappa}{\kappa + w_{ss}\left(1-e^{-D/w_{ss}}\right)}\right], & \pi < \theta < 2\pi \end{cases} \tag{13a, 13b}$$

where $\phi_{ss}$ and $w_{ss}$ denote the steady-state values for the temperature and the volumetric flow rate, respectively. Substituting Eqs. (13a) and (13b) into the momentum Eq. (9), with $dw/d\tau = 0$ yields the following algebraic equation for $w_{ss}$:

$$\left(w_{ss} + \frac{1}{2}\kappa\right)^2 = \frac{(w_{ss} + \kappa)(D + \kappa\,\phi_{in})\left(1 + e^{-D/w_{ss}}\right)}{4\,w_{ss}\left[\kappa + w_{ss}\left(1-e^{-D/w_{ss}}\right)\right]\left[1 + \left(D/\pi\,w_{ss}\right)^2\right]} \tag{14}$$

$$+ \frac{1}{2}\left[1 - \kappa(w_{ss} + \frac{1}{2}\kappa)\right]$$

For no throughflow $\kappa = 0$, Eqs. (13) and (14) reduce to the results for the closed thermosyphon (cf. [ 3, 9 ])*.

The system efficiency, $\eta$, is defined as the ratio of the energy carried away by the throughflow to the total energy added to the loop. At steady state conditions this is given by

$$\eta_{ss} = \frac{\rho\kappa^* c\left[T(2\pi) - T_{in}\right]}{\int_{\pi}^{2\pi} F 2\pi r\, R d\theta} \tag{15}$$

which in dimensionless form is

$$\eta_{ss} = \frac{\kappa}{D}\left[\phi(2\pi) - \phi_{in}\right] \tag{16}$$

Note that for the transient condition the efficiency is

$$\eta = \frac{\kappa}{D}\left[\phi(2\pi,\tau) - \phi_{in}\right] \tag{17}$$

---

*Creveling, et al [ 3 ] obtained an approximate solution for small values of D for a closed toroidal loop.

Transient and Stability Solutions

The coupled, time dependent governing equations, Eqs. (9), (10a) and (10b) have been solved numerically by using a finite difference method to calculate the temperature and the volumetric flow rate variations. The backward difference formula was used in the spatial derivatives and the forward difference formula was used in the time derivatives. The integral in the momentum equation, Eq. (9), was evaluated by using the trapezoidal rule. The governing equations in finite difference form are given by:

$$w_{n+1} = w_n(1-\Gamma\Delta\tau) - \frac{1}{2}\Gamma\kappa\Delta\tau + \frac{\pi}{4}\frac{\Gamma}{D}\left\{\frac{1}{2}\phi_{o,n+1}\cos(0) + \sum_{i=1}^{M-1}\phi_{i,n+1}\cos(i\Delta\theta) + \frac{1}{2}\phi_{M,n+1}\cos(M\Delta\theta)\right\}\Delta\theta\Delta\tau \tag{18}$$

$$\phi_{i,n+1} = \phi_{i,n}\left(1-2D\Delta\tau-2\pi w_n\frac{\Delta\tau}{\Delta\theta}\right) + 2\pi w_n\phi_{i-1,n}\frac{\Delta\tau}{\Delta\theta}, \quad 0 < \theta < \pi \tag{19}$$

$$\phi_{i,n+1} = \phi_{i,n}\left[1-2\pi(w_n+\kappa)\frac{\Delta\tau}{\Delta\theta}\right] + 2\pi(w_n+\kappa)\phi_{i-1,n}\frac{\Delta\tau}{\Delta\theta} + 2D\Delta\tau \quad ; \pi < \theta < 2\pi \tag{20}$$

where $\theta = i\Delta\theta$, $2\pi = M\Delta\theta$ and $\tau = n\Delta\tau$. The initial conditions are specified and the boundary conditions are given by:

$$\phi_{o,n+1} = \phi_{2\pi,n+1} \tag{21}$$

and

$$\phi_{\pi^+,n+1} = \frac{w_{n+1}}{w_{n+1} + \kappa} \phi_{\pi^-,n+1} + \frac{\kappa}{w_{n+1} + \kappa} \phi_{in} \tag{22}$$

Several cases of initial conditions were treated, as discussed later.

The time and space intervals were chosen so as to satisfy the stability criteria of the finite difference equations which are given by:

$$1 - \Gamma\Delta\tau \geq 0 \tag{23}$$

$$1 - 2D\Delta\tau - 2\pi w_n \frac{\Delta\tau}{\Delta\theta} \geq 0 \tag{24}$$

and

$$1 - 2\pi(w_n + \kappa) \frac{\Delta\tau}{\Delta\theta} \geq 0 \tag{25}$$

A time increment of 0.005 was used and a space increment of $\Delta\theta$ equal to $2\pi/80$ was chosen.

The numerical formulation, Eqs. (18)-(22), was also used to investigate the stability characteristics of the natural circulation flows in the loop. For this part of the study the equations were solved with initial conditions corresponding to small perturbations of the (known) steady state flows. Stability was determined by the behavior of the solutions, i.e., the growth or decay of the perturbations.

## RESULTS AND DISCUSSION

The transient, steady-state and stability behavior of a thermosyphon with throughflow has been investigated. Numerical calculations were started at time $\tau = 0$ for a specified initial volumetric flow rate, $w_i$, and temperature distribution, $\phi_i$, of the circulating fluid. The volumetric flow rate, $\kappa$, and inlet temperature, $\phi_{in}$, of the injected fluid (throughflow) have been taken as constant. The circulating and the injected fluid are assumed to be mixed perfectly at $\theta = \pi$, the inlet to the heating region. The same amount of injected fluid is withdrawn at $\theta = 2\pi$ which is the outlet from the heating region. The remaining fluid cools in the upper region, $0 < \theta < \pi$ by convection to the cold wall which is maintained at a constant temperature (cf. Fig. 1).

Typical results for the temperature are shown in Figs. 2a and 2b for values of $\Gamma = 1$, $D = 2.5$, an initial temperature profile $\phi_i = 0$, an initial volumetric flow rate $w_i = 1.5$, a volumetric throughflow rate $\kappa = 0.2$ and different inlet temperature of the throughflow, $\phi_{in} = -0.5$ and 0. It is pointed out that the condition of initial flow with a uniform temperature ($\phi_i = 0$) corresponds to forced flow in the loop (driven by a pump) before activation of the heater. It can also represent, approximately, a strong forced flow with respect to the input power, where the temperature differences are small. This initial condition may be encountered during nuclear reactor power plant cooling after a reactor scram and the pumps trip. Other types of boundary conditions, e.g., initiation of flow from rest, have also been studied [12,17] and also perturbations from the steady state condition (cf. Figs. 7-9). The variations of the volumetric flow rate, w, are shown in Figs. 3a and 3b for the cases $\phi_{in} = 0$ and -0.5 for initial volumetric flow rates, ranging from $w_i = 0.2$ to 1.5.

For small times, there is a thermal penetration depth in the cooled region ($0 < \theta < \pi$) beyond which there is no heating effect (that is, $\partial\phi/\partial\theta = 0$, cf. Figs. 2a and 2b). Similarly, there is a penetration depth in the heated region ($\pi < \theta < 2\pi$) beyond which $\partial\phi/\partial\theta = 0$, cf. Figs. 2a and 2b. These results may also be deduced from the formal solution to equations (10a) and (10b) for small times which are presented in the Appendix. Comparing the results for the penetration depth, $\theta_p$, with those of [9] for a closed loop, $\kappa = 0$, it is concluded that the throughflow tends to slightly reduce $\theta_p$. (Also refer to Figs. 3a and 3b which explicitly show for $w_i = 0.6$ that the velocity is less for the throughflow case. In the Appendix it is shown that smaller velocities yield smaller penetration depths.) It is also seen that there is a discontinuity in the temperature at $\theta = \pi$ which results from the assumption of perfect mixing at this location of the circulating fluid with the injected fluid (throughflow).

Results for larger times, as well as for smaller times are shown in Figs. 2a and 2b for the temperature and in Figs. 3a and 3b for the volumetric flow rate (for initial volumetric flow rates, ranging from $w_i = 0.2$ to 1.5). For completeness, it is noted that results for the closed loop, $\kappa = 0$, (Greif, Zvirin and Mertol [9]) have larger flow rates than those obtained for the throughflow case for the condition $\kappa = 0.2$ for both $\phi_{in} = 0$ and -0.5.

The temporal variation of the temperature is shown in Figs. 4a and 4b at three locations, $\theta = 0$, $\pi/2$ and $3\pi/2$. For all the cases considered, the flow rate initially decreases (cf. Figs. 3a and 3b). For $w_i = 0.2$, 0.6 and 0.8 this initial decrease causes the velocity to differ (for small times) from the steady state value, $w_{ss} = 0.814$. This is accompanied

by an overshoot of the temperature; that is, $\phi/\phi_{ss} > 1$, with the greatest effects occurring when the flow rate is small and the heating of the fluid is therefore more prolonged and effective. Note that there is a small flow overshoot for $w_i = 0.2$ (cf. Fig. 3b). A comparison of the closed loop ($\kappa = 0$) and the present loop with throughflow is made in Fig. 3b. For $w_i = 0.6$ the closed loop has a flow overshoot while the loop with throughflow has no overshoot.

The steady state values of the flow rate, $w_{ss}$, and the temperature, $\phi_{ss}$, are given in Table 1. Note in Figs. 4a ($\phi_{in} = 0$) and 4b ($\phi_{in} = -0.5$) that the temperatures with throughflow are lower than for the closed loop, $\kappa = 0$ (the comparison is shown for $w_i = 0.6$).

In Figs. 5a ($\phi_{in} = -0.5$) and 5b ($\phi_{in} = 0$) the variations of the efficiency with time are shown for different initial flow rates, $w_i$. From the definition of the efficiency, Eq. (17), we have that the only time dependent quantity is the temperature $\phi(2\pi,\tau)$. Accordingly, the shape of the curves follows directly from the previous discussion; the rate of increase of the efficiency being greatest (and in fact, linear) for small times when the flow rate is decreasing. In Fig. 6 the efficiency is plotted for one flow rate, $w_i = 1.5$, for three values of the inlet temperature, $\phi_{in} = -0.5, 0, 0.5$ and for volumetric throughflow rates, ranging from $\kappa = 0.2$ to 1.0. For small times, there is some crossing over of the curves but for larger times the efficiency increases for increasing values of the volumetric throughflow rate and for decreasing values of the inlet temperature. These trends may also be noted in the steady state tabulation of the efficiencies, Table 1.

The above results correspond to flows which approach the steady state values and are denoted as stable flows. There are, however, unstable cases when the flow and temperature oscillate with increasing amplitude (cf. Figs. 7 and 8) as well as neutrally stable cases where the magnitude of the oscillations about the steady-state values remain constant (cf. Fig. 9).

In the absence of a throughflow, the instabilities in the toroidal loop have been studied experimentally [3,4] and theoretically [3,4,9,10]. It is generally believed that these instabilities are caused by phase shifts between the buoyancy (driving) forces created by temperature differences, and the friction forces (or flow rates). Such a phenomenon can occur when a "pocket" of fluid at a temperature higher than usual enters the heating region at a flow rate lower than usual. The pocket will then be heated to a much higher value (due to its smaller velocity), and if it cannot be adequately cooled down it will reenter the heating region at a still higher temperature and the process will be repeated and amplified. A stability map is shown in Fig. 10 for $\phi_{in} = 0$ and 0.5, respectively.

In Fig. 10 the effect of throughflow, $\kappa$, is seen to increase the stability of the loop since some perturbations which would cause instability (for $\kappa = 0$) are now carried out of the loop with the throughflow. The stable portion of the graph is therefore increased, that is, the neutrally stable curve shifts to the left for increasingly larger values of $\kappa$. The cooler inlet case, $\phi_{in} = 0$, yields lower temperatures; hence, less buoyancy and smaller velocities result, and consequently a more stable system is obtained. It is noted that the cool inlet case $\phi_{in} = -0.5$ was completely stable for the range of values of Fig. 10.

The steady state behavior is obtained from the analytical solutions, Eqs. (13) and (14). In general, Eq. (14) must be solved numerically to obtain the steady state flow rate, $w_{ss}$, which depends on the system parameter D and the throughflow conditions $\kappa$ and $\phi_{in}$. Once $w_{ss}$ is known, the steady-state temperatures, $\phi_{ss}$, can be calculated from Eq. (13).

The steady-state values are summarized in Table 1 and in Fig. 11. An interesting result, namely, the existence of multiple steady-state solutions is obtained for small values of D (cf. Fig. 11). The existence of multiple solutions implies metastable equilibrium and a finite amplitude mode of instability. This differs from the small amplitude instabilities associated with oscillatory motion which were previously discussed. The multiple solutions can be explained as follows. At steady state the frictional resistance is balanced by the driving buoyancy force. While the former is a monotonically increasing function of the flow rate, $w_{ss}$, (linear in our case), the latter is a complicated function of $w_{ss}$ (cf. Eq. (9) with $d/d\tau = 0$) which has one or two extremum. The result is that there are sometimes cases where there are two and even three values of $w_{ss}$ for which the two forces are balanced. It is noted that multiple solutions have been obtained by Damerell and Schoenhals [4] for a toroidal asymmetrical loop and by Zvirin [18] for the vertical loop with point heat source and sink.

As mentioned above, the steady state flow rate, $w_{ss}$, must, in general, be solved numerically from Eq. (14). It is possible, however, to obtain simpler relations for limiting values of the parameters which yield results that are in agreement with Fig. 11. In detail, for large values of D Eq. (14) reduces to

$$w_{ss} \approx (\tfrac{1}{4}) \left(-3\kappa + \sqrt{\kappa^2 + 8}\right) + O(1/D), \quad D \gg 1 \tag{26}$$

Thus, only single steady-state solution exist in this range. For small values of D and $D/w_{ss}$, Eq. (14) reduces to the cubic equation

$$2 w_{ss}^3 + 3\kappa w_{ss}^2 + [\kappa^2 - 1 - \frac{D + \kappa\phi_{in}}{D + \kappa}] w_{ss} - \kappa \frac{D + \kappa\phi_{in}}{D + \kappa} = 0, \qquad (27)$$

$$D << 1 \text{ and } D/w_{ss} << 1$$

For D = 0.01, $\kappa$ = 0.1 and $\phi_{in}$ = -0.5, values of $w_{ss}$ equal to 0.453 and 0.0605 are obtained which agree with the results shown in Fig. 11. Note that the third steady state result for this condition cannot be obtained from Eq. (27) because it does not satisfy the constraint, $D/w_{ss} << 1$. However, the third result may be obtained from the solution to the following equation

$$w_{ss}^2 + (\frac{3\kappa}{2} - \frac{\pi^2}{4} \cdot \frac{D + \kappa\phi_{in}}{D^2}) w_{ss} + \frac{1}{2} (\kappa^2 - 1) = 0, \qquad (28)$$

$$D << 1 \text{ and } D/w_{ss} >> 1$$

which yields a value of $w_{ss} = 5.00 \times 10^{-4}$, in agreement with the result shown in Fig. 11.

Detailed stability calculations were carried out for the case D = 0.1 and $\phi_{in}$ = 0.5, and for the upper portion of the $w_{ss}$ vs. $\kappa$ curve in Fig. 11 stable results were obtained for both small and large values of D in agreement with Fig. 11. However, for the lower portion of the $w_{ss}$ vs. $\kappa$ in Fig. 11 these solutions always exhibited unstable behavior for all the values of D that were used. Note that for these calculations, the very small values of the velocity (cf. Fig. 11) in conjunction with the initial decrease in the velocity (cf. Figs. 3a and 3b) lead to negative values of the velocity and this flow reversal denotes an unstable condition.

REFERENCES:

(1) Keller, J.B., "Periodic Oscillations in a Model of Thermal Convection", J. Fluid Mech., Vol. 26, 1966, pp. 599-606.

(2) Welander, P., "On the Oscillatory Instability of a Differentially Heated Fluid Loop", J. Fluid Mech., Vol. 29, 1967, pp. 17-30.

(3) Creveling, H.F., De Paz, J.F., Baladi, J.Y., and Schoenhals, R.J., "Stability Characteristics of a Single-Phase Free Convection Loop", J. Fluid Mech., Vol. 67, 1975, pp. 65-84.

(4) Damerell, P.S., and Schoenhals, R.J., "Flow in a Toroidal Thermosyphon with Angular Displacement of Heated and Cooled Sections", J. Heat Transfer, Vol. 101, 1979, pp. 672-676.

(5) Zvirin, Y., Shitzer, A., and Grossman, G., "The Natural Circulation Solar Heater-Models with Linear and Nonlinear Temperature Distributions", Int. J. Heat Mass Transfer, Vol. 20, 1977, pp. 997-999.

(6) Zvirin, Y., Shitzer, A., and Bartal-Bornstein, A., "On the Stability of the Natural Circulation Solar Heater", in Proceedings of the 6th International Heat Transfer Conference, Toronto, Canada, Vol. 2, 1978, pp. 141-145.

(7) Mertol, A., Place, W., Webster, T., and Greif, R., "Thermosiphon Water Heaters with Heat Exchangers", AS/ISES Conference, Phoenix, Arizona, June 2-6, 1980 (Lawrence Berkeley Laboratory Report, LBL-10033, 1980).

(8) Mertol, A., Place, W., Webster, T., and Greif, R., "Detailed Loop Model (DLM) Analysis of Liquid Solar Thermosiphons with Heat Exchangers", Lawrence Berkeley Laboratory Report, LBL-10699, 1980.

(9) Greif, R., Zvirin, Y., and Mertol, A., "The Transient and Stability Behavior of a Natural Convection Loop", J. Heat Transfer, Vol. 101,

1979, pp. 684-688.

(10) Mertol, A., "Heat Transfer and Fluid Flow in Thermosyphons", Ph.D Thesis, University of California, Berkeley, 1980.

(11) Japikse, D., "Advances in Thermosyphon Technology", in Advances in Heat Transfer, edited by Irvine, T.F., Jr., and Hartnett, J.P., Vol. 9, Academic Press, New York, 1973, pp. 1-111.

(12) Zvirin, Y., and Greif, R., "Transient Behavior of Natural Circulation Loops: Two Vertical Branches with Point Heat Source and Sink", Int. J. Heat Mass Transfer, Vol. 22, 1979, pp. 499-504.

(13) Zvirin, Y., Jeuck III, P.R., Sullivan, C.S., and Duffey, R.B., "Experimental and Analytical Investigation of a PWR Natural Circulation Loop", ANS/ENS Thermal Reactor Safety Meeting, Knoxville, Tenn., April 1980.

(14) Ong. K.S., "A Finite Difference Method to Evaluate the Thermal Performance of a Solar Water Heater", Solar Energy, Vol. 16, 1974, pp. 137-147.

(15) Ong, K.S., "An Improved Computer Program for the Thermal Performance of a Solar Water Heater", Solar Energy, Vol. 18, 1976, pp. 183-191.

(16) Torrance, K.E., "Open-Loop Thermosyphons with Geological Applications", J. Heat Transfer, Vol. 101, 1979, pp. 677-683.

(17) Zvirin, Y., "Throughflow Effects on the Transient and Stability Characteristics of a Thermosyphon", in Advanced Energy Systems Which Maintain the Atmospheric $CO_2$ Balance, edited by C.W. Solbrig, Science Press, 1980.

(18) Zvirin, Y., "The Effects of a Throughflow on the Steady State and Stability of a Natural Circulation Loop", 19th National Heat Transfer Conference, Orlando, Florida, July 1980.

# APPENDIX

## Solution for Small Time and Determination of the Thermal Penetration Depth

A formal solution of the energy equation, eq. (10) may be obtained for small times and this will yield the "thermal penetration depth." From the theory of characteristics for $2\pi \int_0^\tau w(\bar{\tau})d\bar{\tau} < \pi$ the temperature is given by:

$$\phi(\theta,\tau) = \left\{ \begin{array}{ll} 0 \quad \text{for} \quad \theta \geq \theta_p & \\ e^{-2D\tau} \, \text{fcn}_I \left[ 2\pi \int_0^\tau w(\bar{\tau})d\bar{\tau} - \theta \right] & \text{for } \theta < \theta_p \end{array} \right\} \text{for } 0 \leq \theta \leq \pi^- \quad \text{(A-1)}$$

For $2\pi \int_0^\tau w(\bar{\tau})d\bar{\tau} + 2\pi\tau\kappa < \pi$, the temperature is:

$$\phi(\theta,\tau) = \left\{ \begin{array}{ll} 2D\tau \quad \text{for} \quad \theta-\pi \geq \theta_p + 2\pi\tau\kappa & \\ 2D\tau - \text{fcn}_{II}\left[ 2\pi \int_0^\tau w(\bar{\tau})d\bar{\tau} + 2\pi\tau\kappa - (\theta-\pi) \right] & \text{for } (\theta-\pi) < \theta_p + 2\pi\tau\kappa \end{array} \right\} \quad \text{(A-2)}$$

$$\text{for } \pi^+ \leq \theta \leq 2\pi$$

where $\theta_p$, is the thermal penetration depth or thermal signal, is equal to $2\pi \int_0^\tau w(\bar{\tau})d\bar{\tau}$.

It should be noted that the functions in eqs. (A-1) and (A-2) may be obtained by using the conditions that are valid for small time, namely:

$$\phi(0,\tau) = 2D\tau \tag{A-3a}$$

$$\phi(\pi^-,\tau) = 0 \tag{A-3b}$$

and

$$\phi(\pi^+,\tau) = \frac{w(\tau)}{w(\tau) + \kappa} \phi(\pi^-,\tau) + \frac{\kappa}{w(\tau) + \kappa} \phi_{in} \tag{A-3c}$$

so that

$$\text{fcn}_I \left[ 2\pi \int_0^\tau w(\bar{\tau})\, d\bar{\tau} \right] = 2D\tau\, e^{2D\tau} \tag{A-4}$$

and

$$\text{fcn}_{II} \left[ 2\pi \int_0^\tau w(\bar{\tau}) d\bar{\tau} + 2\pi\tau\kappa \right] = 2D\tau - \frac{\kappa}{w(\tau) + \kappa} \phi_{in} \tag{A-5}$$

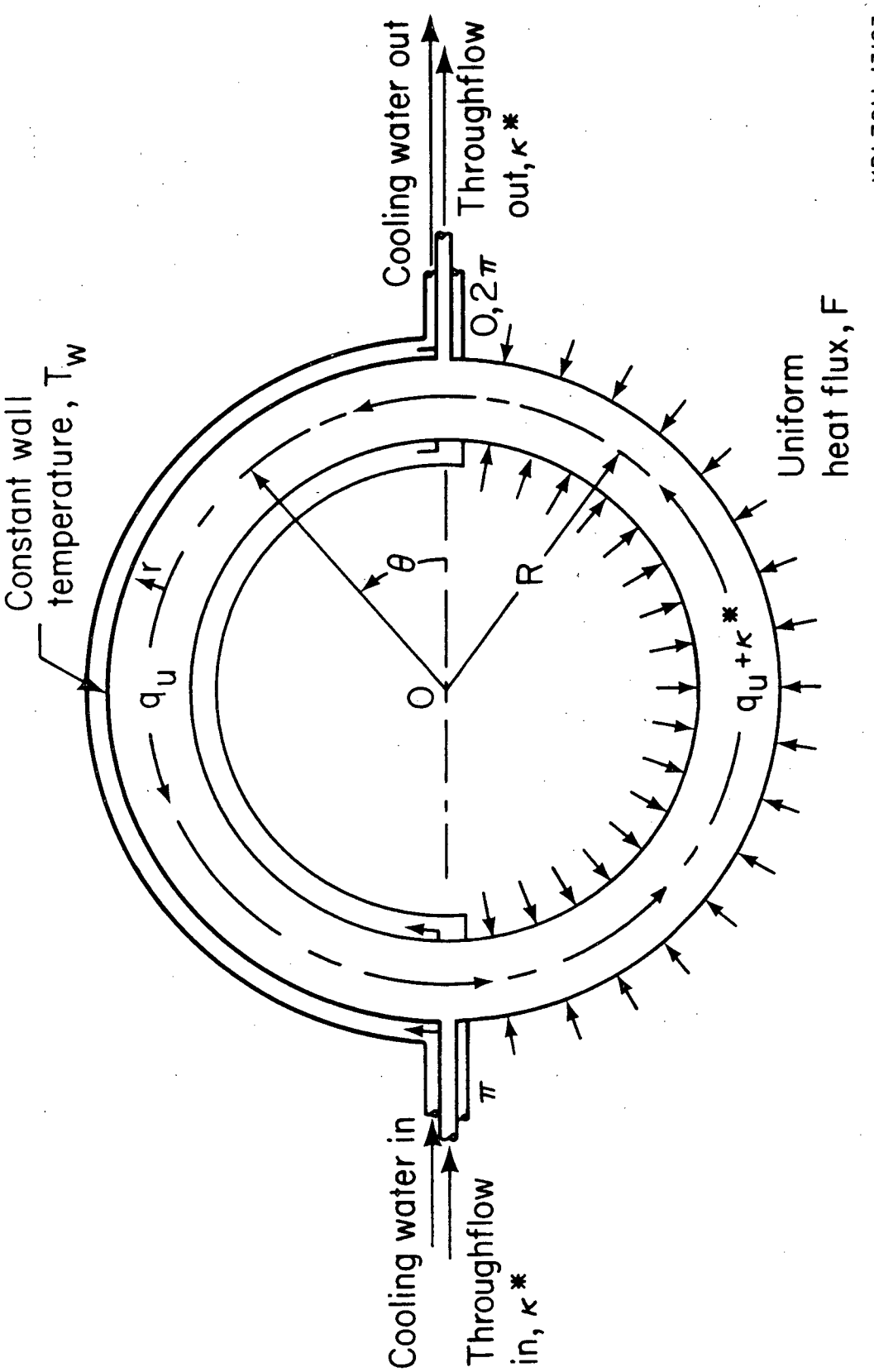


XBL7911-13123

FIGURE 1. Toroidal open thermosyphon.

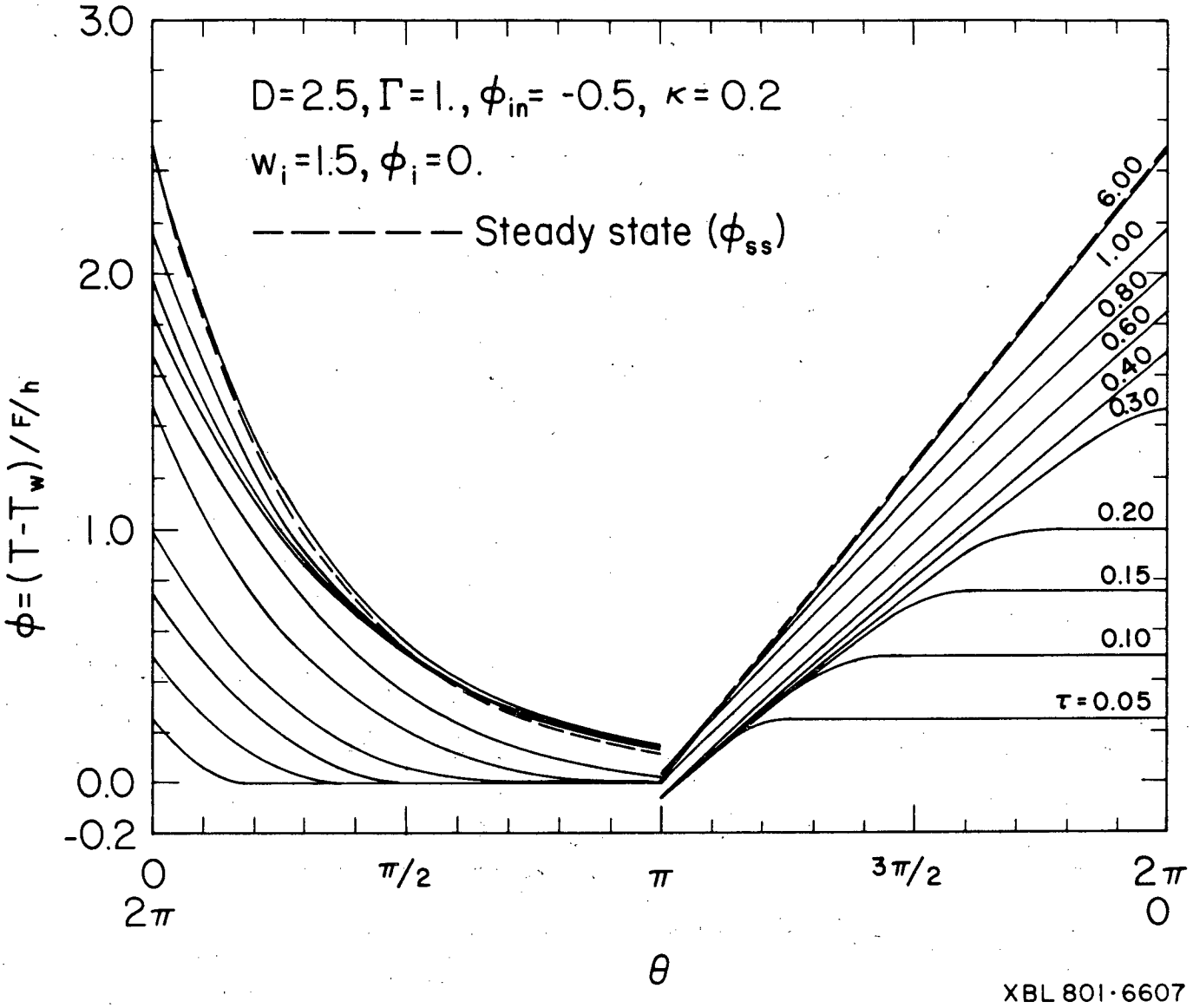


FIGURE 2a. Temperature distribution at different times for stable condition ($\Phi_{in}$ = -0.5).

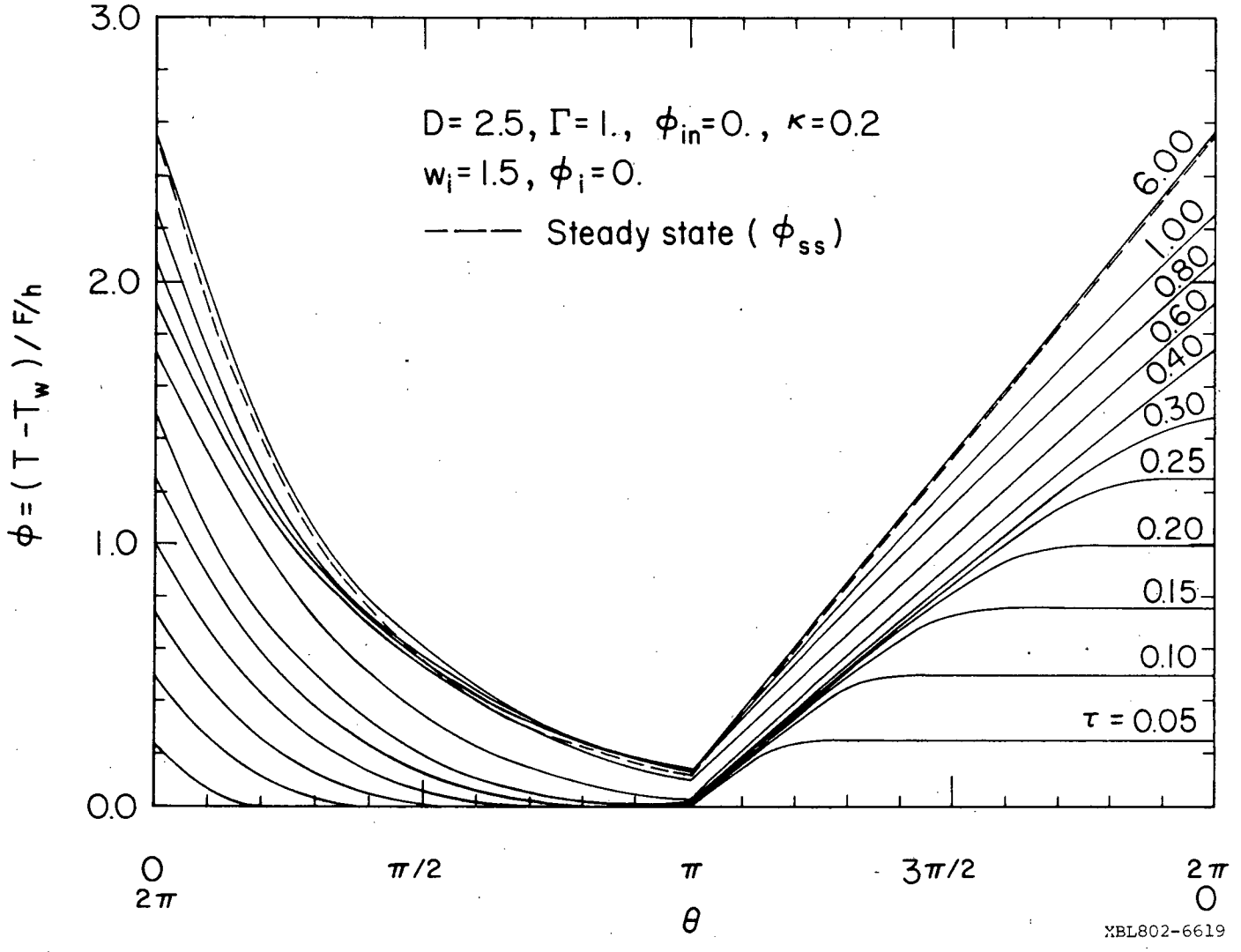


FIGURE 2b. Temperature distribution at different times for stable condition ($\Phi_{in}$ = 0).

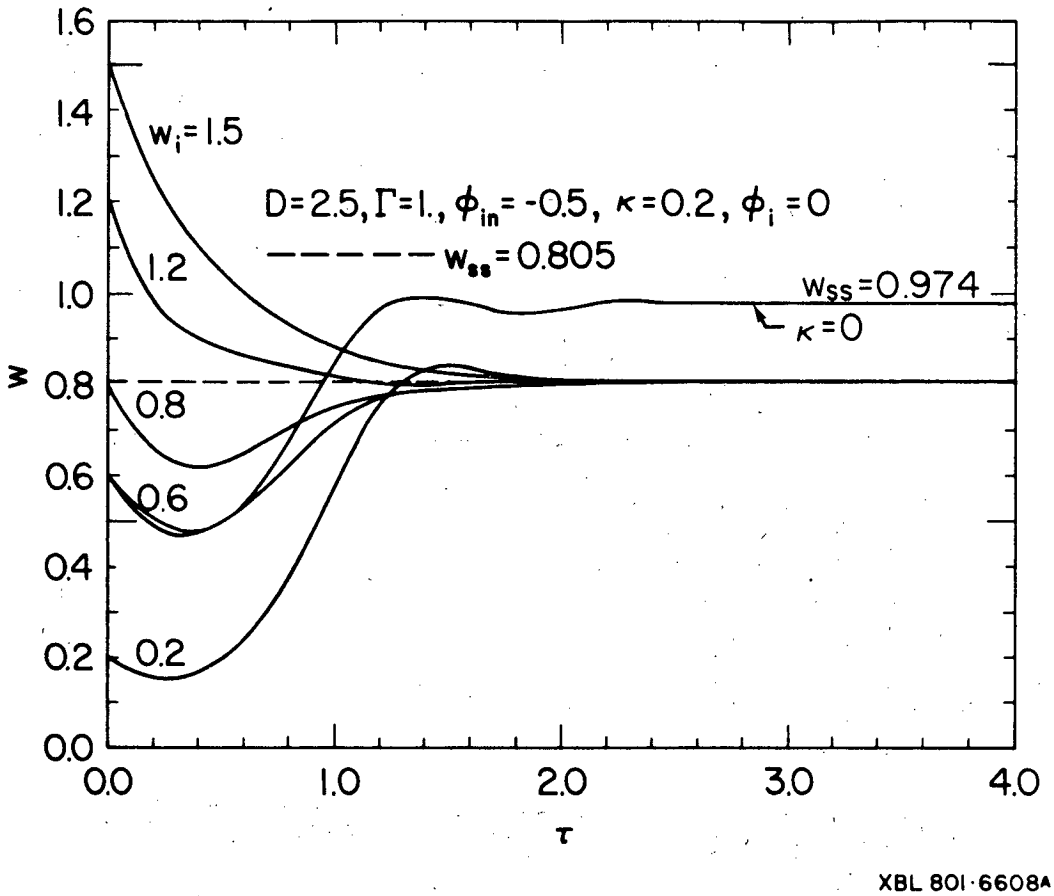


FIGURE 3a. Volumetric flow rate (or velocity) variation for different initial volumetric flow rates for stable condition ($\phi_{in}$ = -0.5).

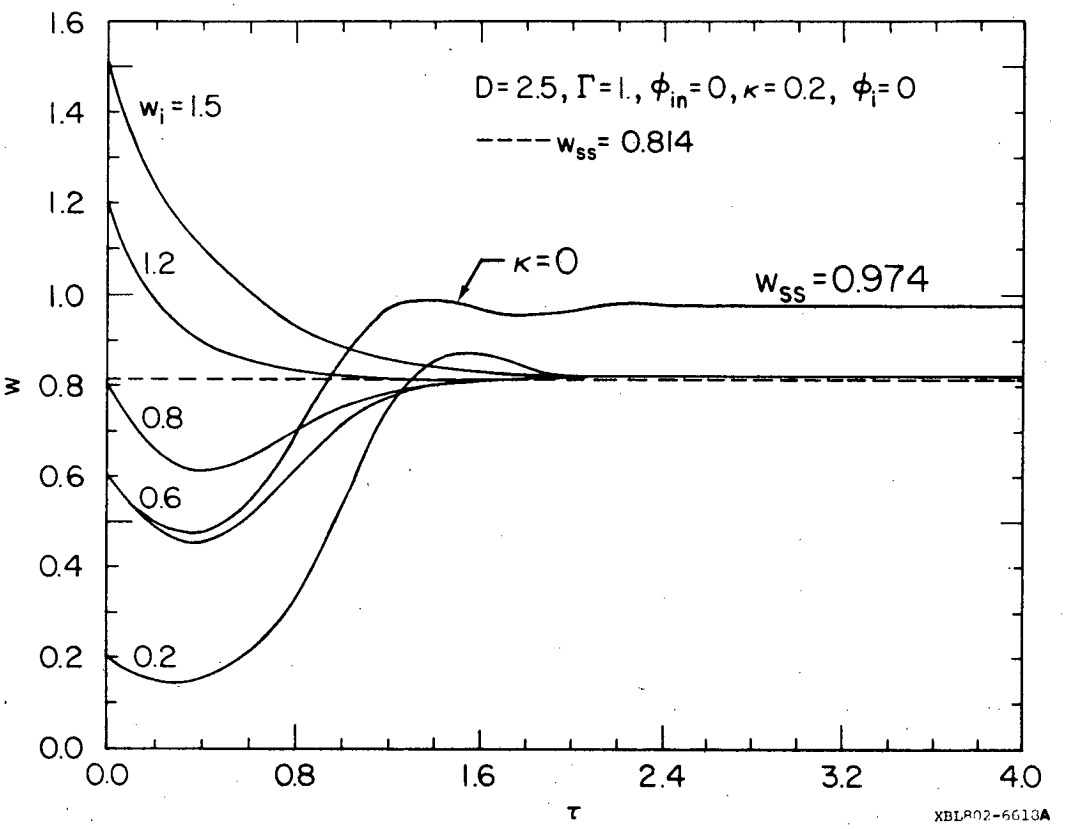


FIGURE 3b. Volumetric flow rate (or velocity) variation for different initial volumetric flow rates for stable condition ($\Phi_{in}$ = 0).

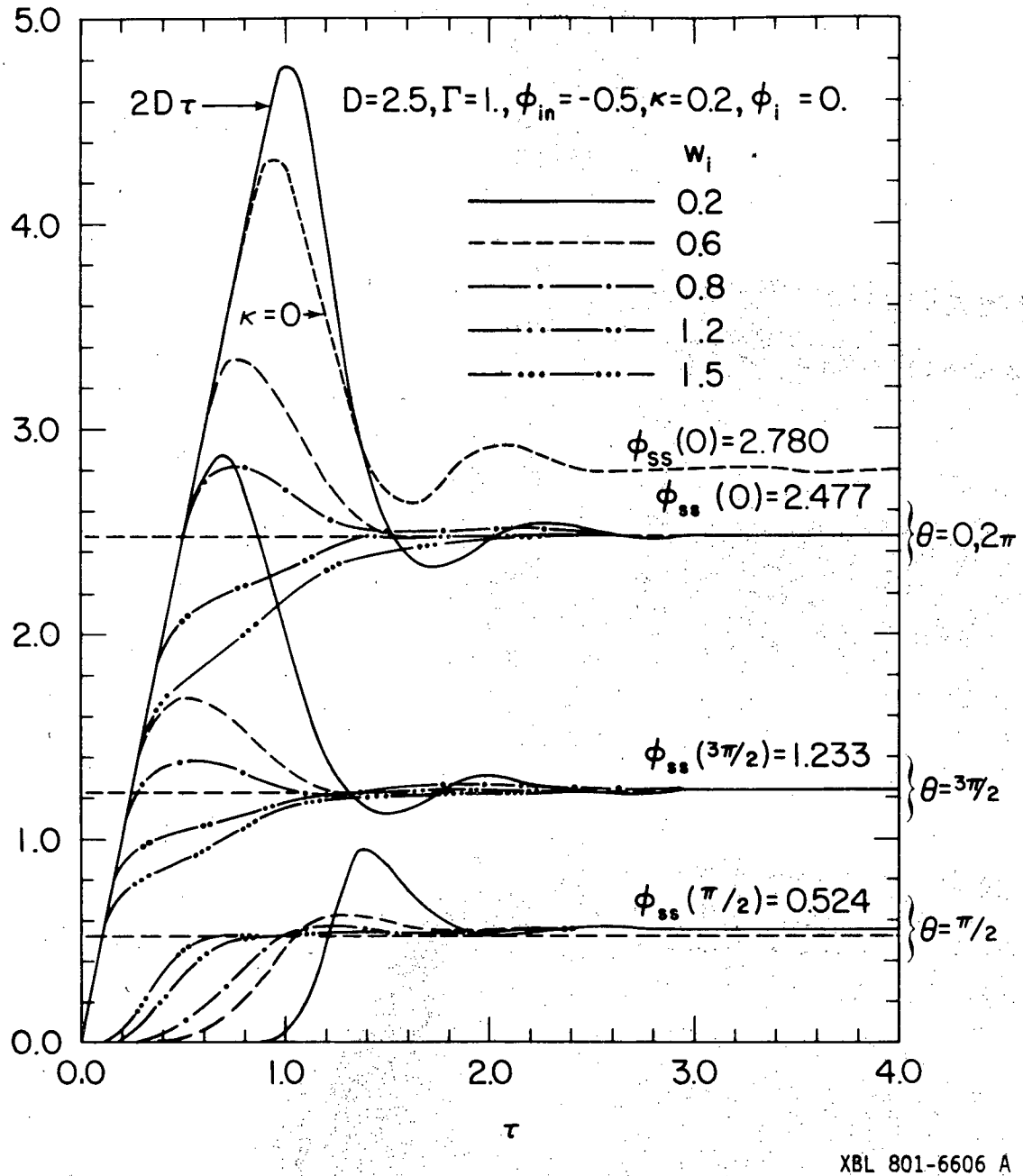


FIGURE 4a. Temperature variations for different initial volumetric flow rates for stable condition ($\Phi_{in}$ = -0.5).

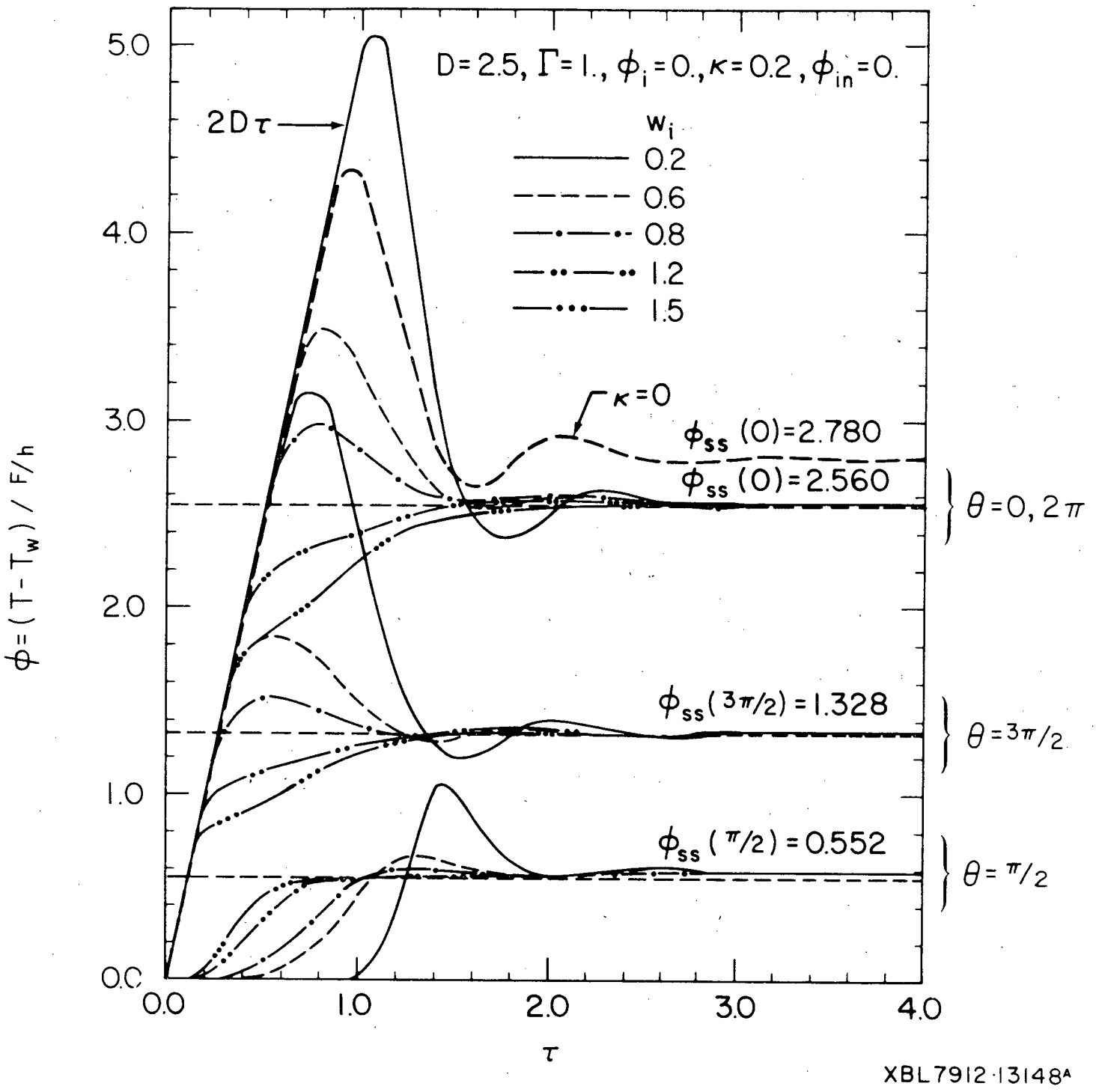


FIGURE 4b. Temperature variations for different initial volumetric flow rates for stable condition ($\Phi_{in}$ = 0).

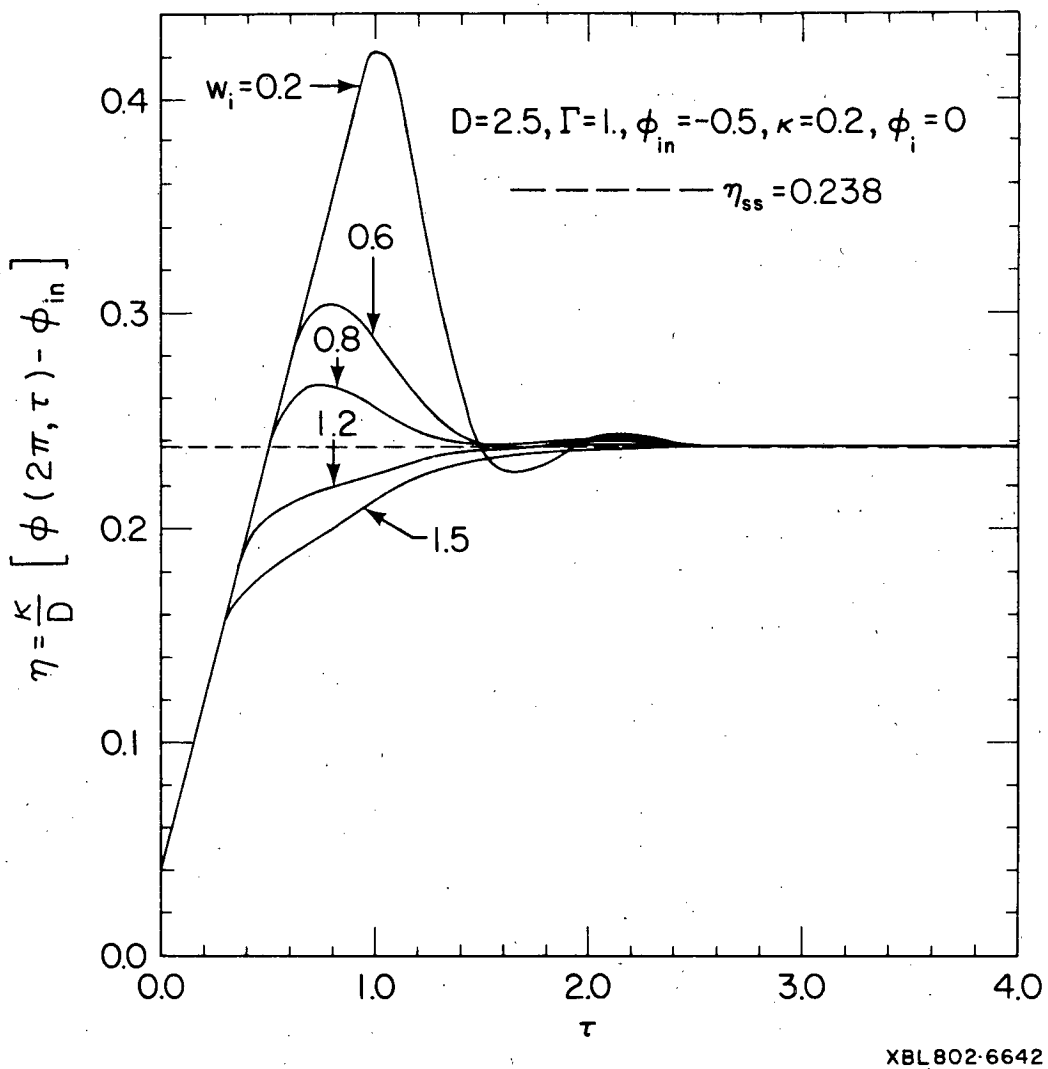


FIGURE 5a. Efficiency variations for different initial volumetric flow rates for stable condition ($\Phi_{in}$ = -0.5).

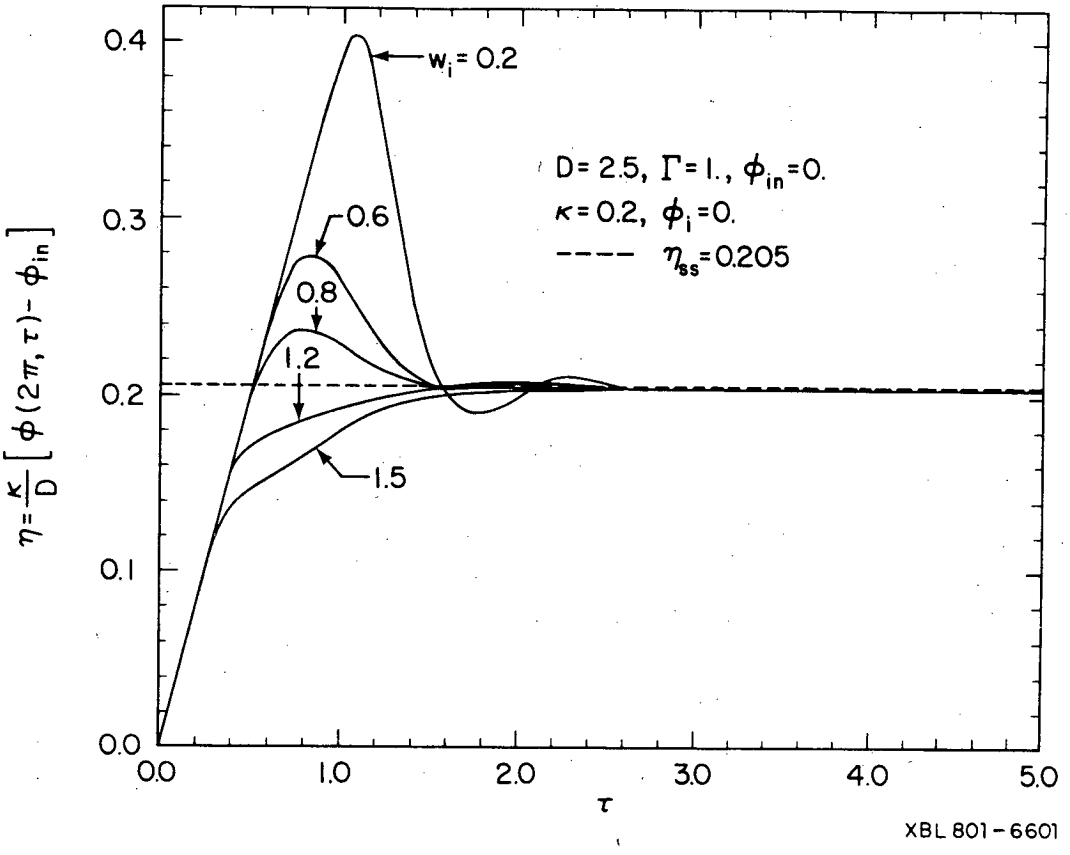


FIGURE 5b. Efficiency variations for different initial volumetric flow rates for stable condition ($\Phi_{in} = 0$).

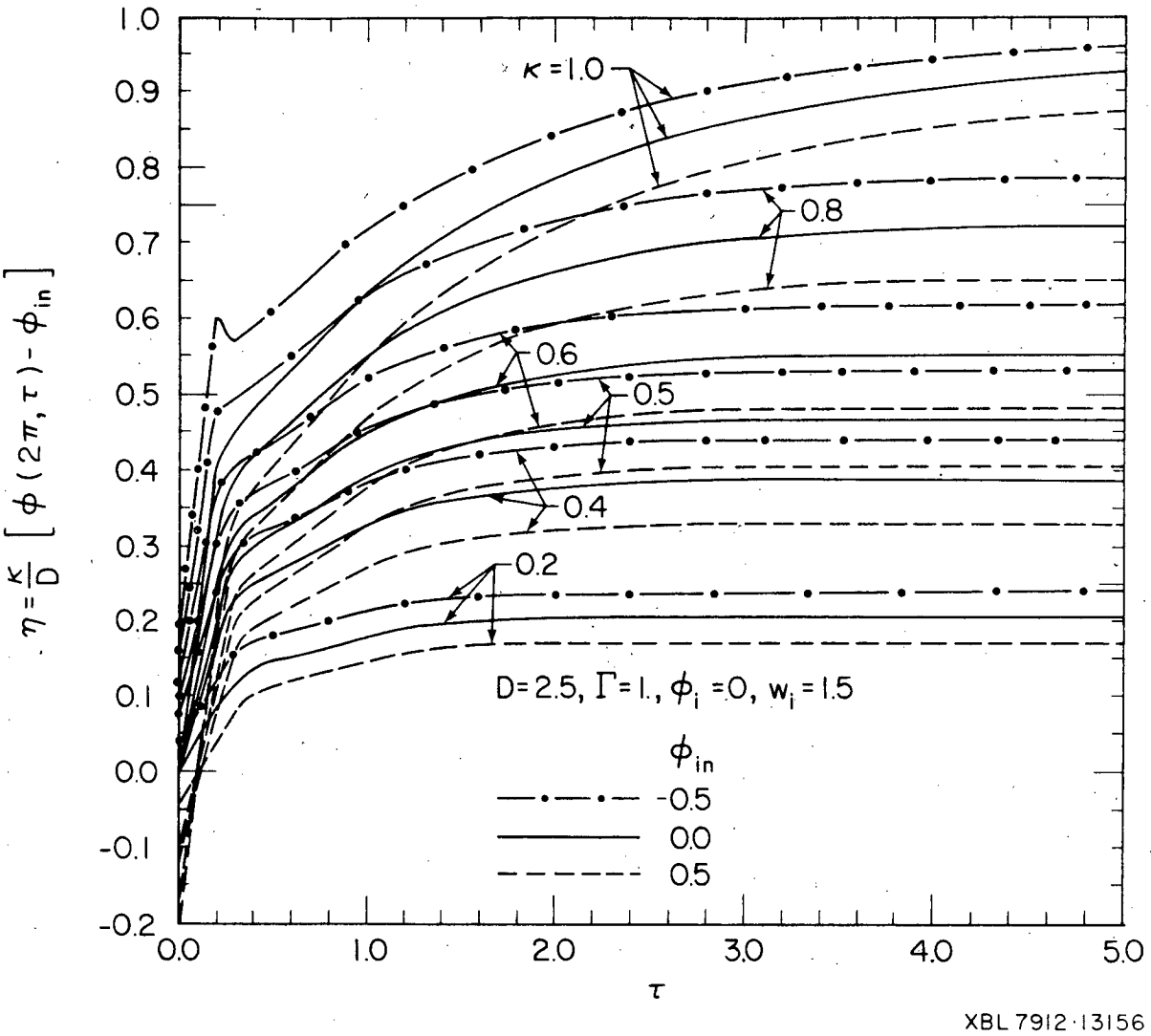


FIGURE 6. Efficiency variations for different volumetric throughflow rates and for different inlet temperatures.

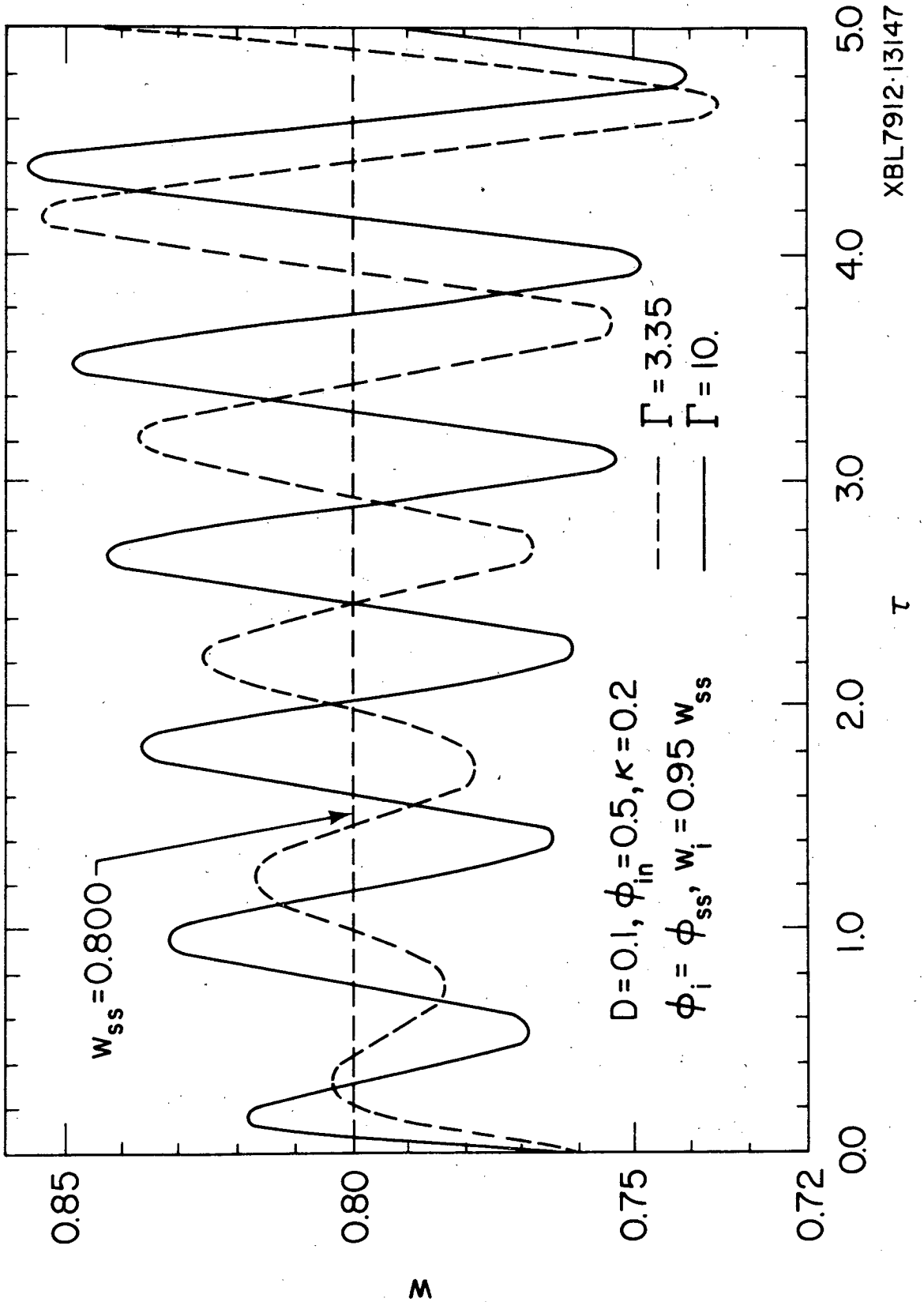


FIGURE 7. Volumetric flow rate (or velocity) variation for unstable conndition.

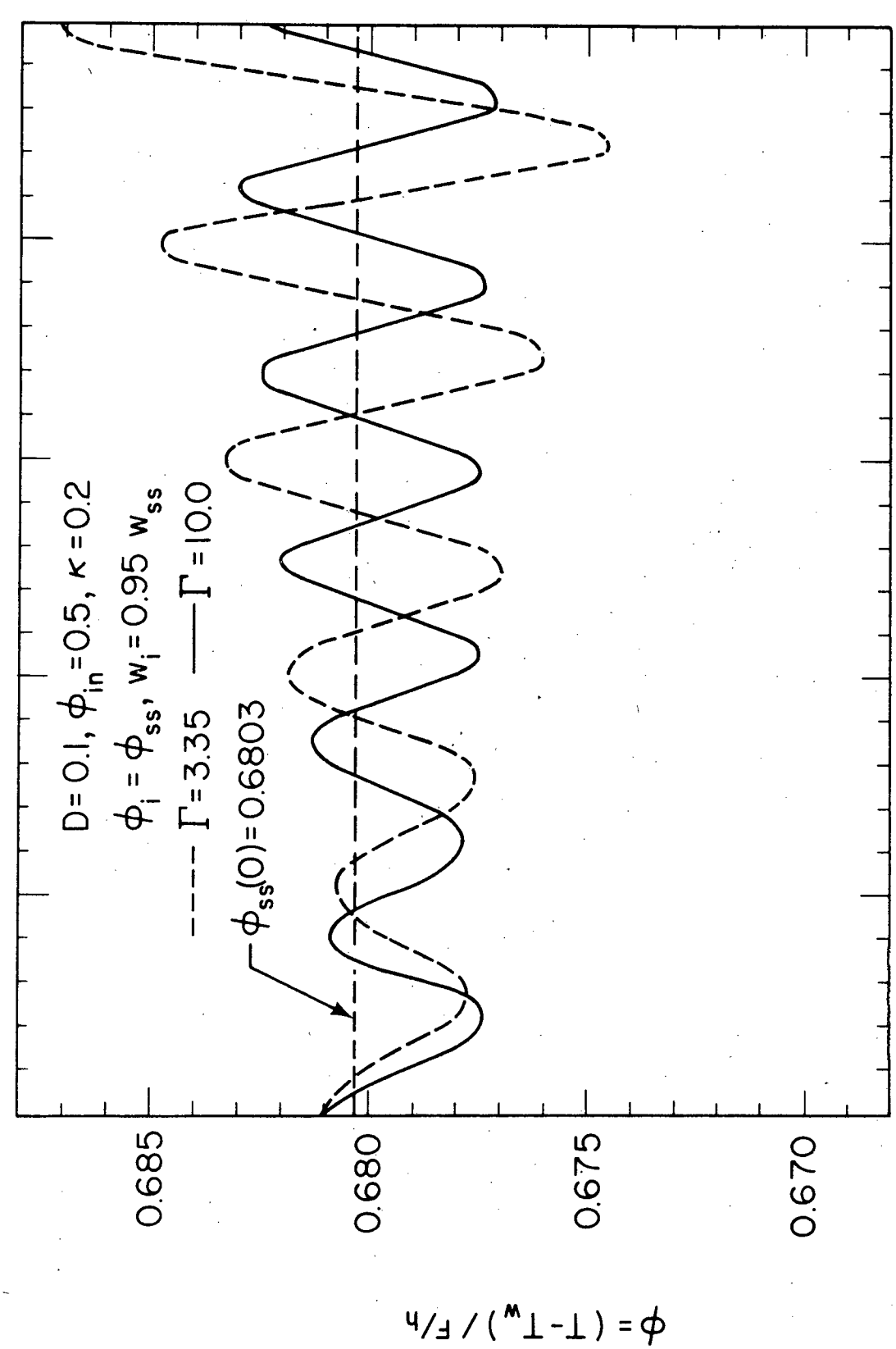


FIGURE 8. Temperature variation for unstable condition.

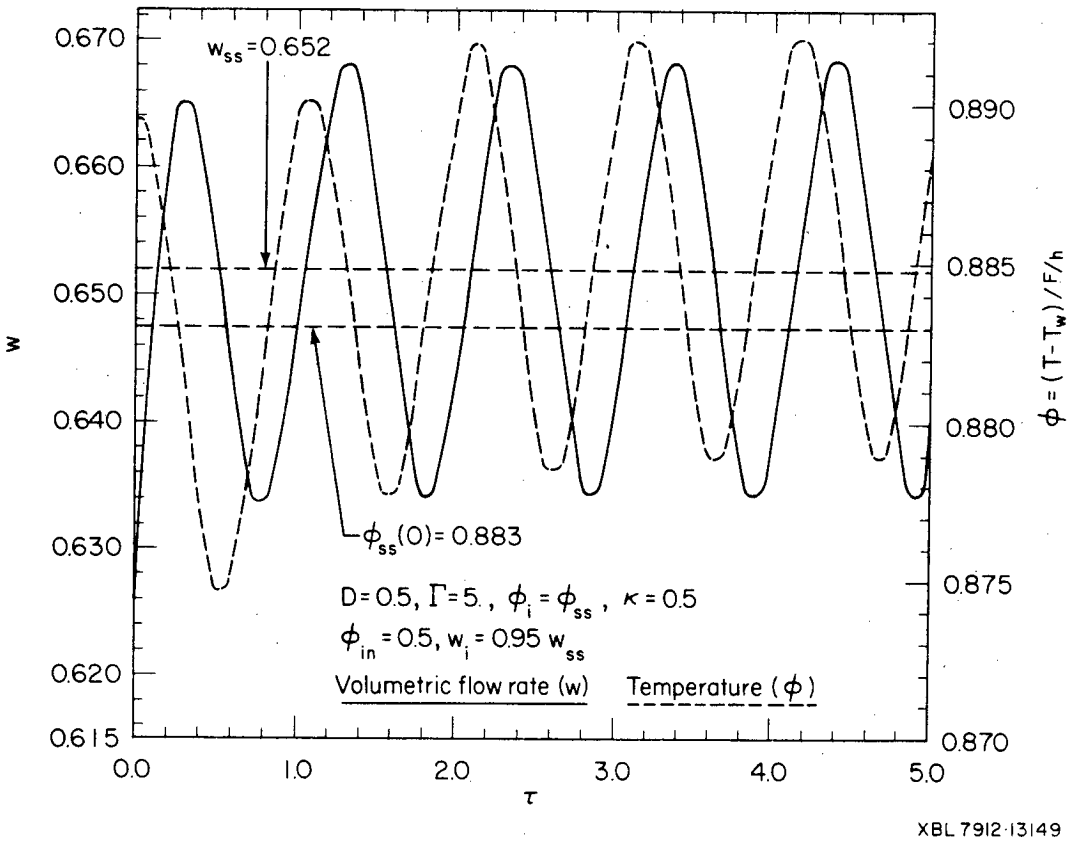


FIGURE 9. Volumetric flow rate (or velocity) and temperature variations for neutrally stable condition.

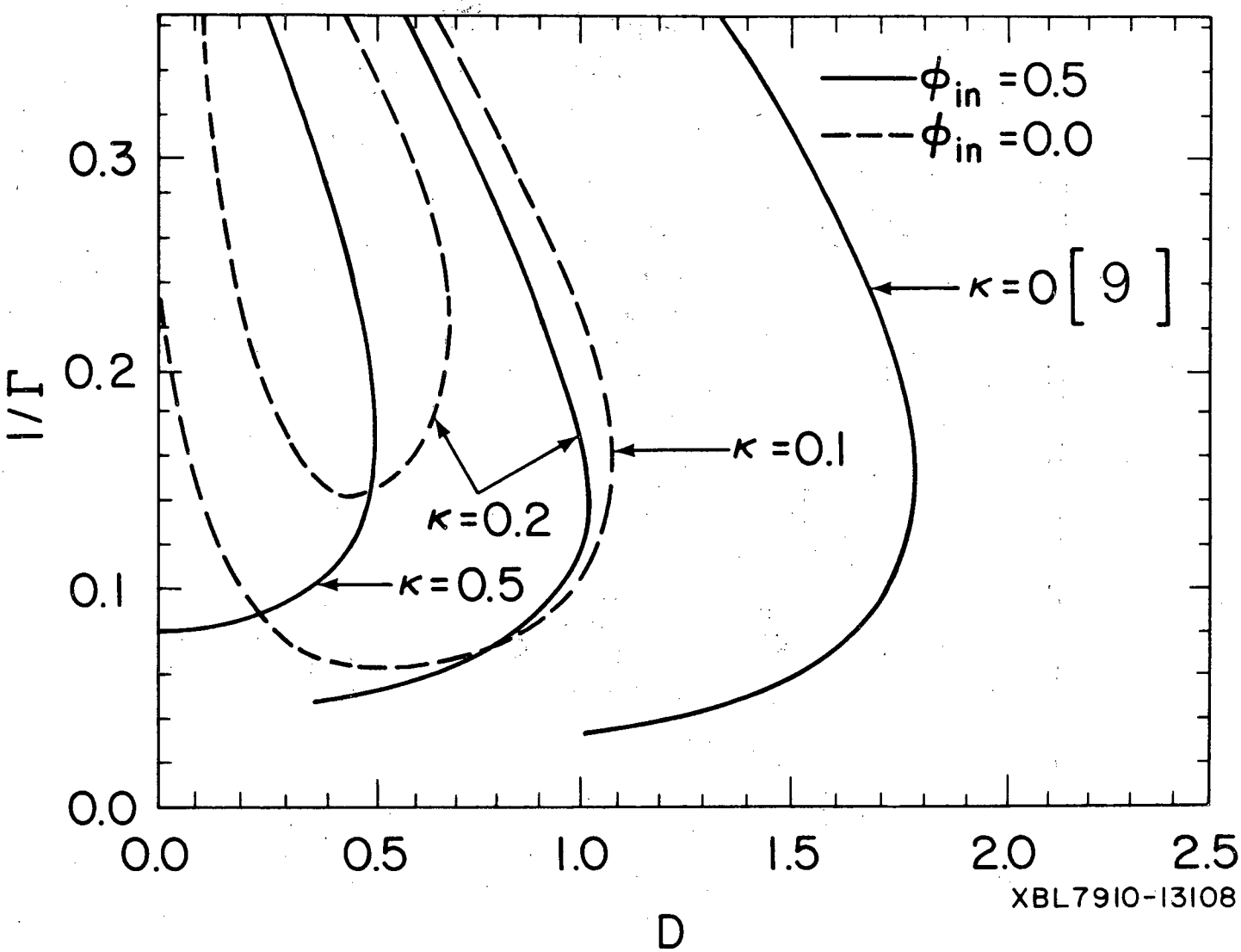


FIGURE 10. Stability map for laminar flow (stable to the right of the neutral stability curve, unstable to the left of the curve).

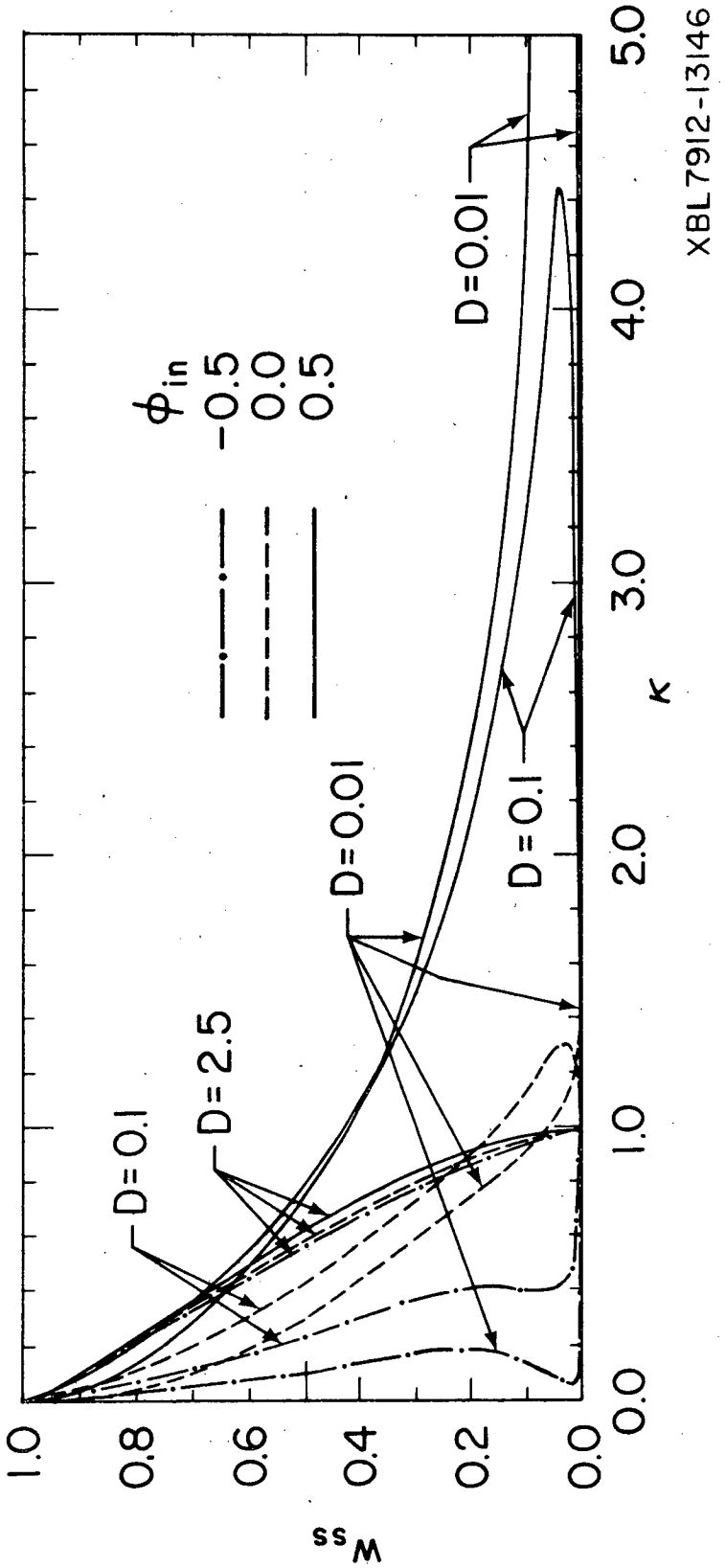


FIGURE 11. Steady-state thermosyphon flow rate versus throughflow rate for different inlet temperatures of throughflow and for different D values.

| D | $\phi_{in}$ | $\kappa$ | $w_{ss}$ | $\phi_{ss}(\theta)$ $\theta=0,2\pi$ | $\theta=\pi/2$ | $\theta=\pi^-$ | $\theta=\pi^+$ | $\theta=3\pi/2$ | $\eta_{ss}$ |
|---|---|---|---|---|---|---|---|---|---|
| 0.1 | -0.5 | 0.0 | 1.000 | 1.051 | 1.000 | 0.951 | 0.951 | 1.000 | 0.000 |
| | | 0.1 | 0.724 | 0.259 | 0.241 | 0.225 | 0.137 | 0.198 | 0.759 |
| | 0.0 | 0.0 | 1.000 | 1.051 | 1.000 | 0.951 | 0.951 | 1.000 | 0.000 |
| | | 0.1 | 0.804 | 0.515 | 0.484 | 0.455 | 0.405 | 0.460 | 0.515 |
| | | 0.5 | 0.448 | 0.170 | 0.152 | 0.136 | 0.064 | 0.117 | 0.848 |
| | | 0.9 | 0.202 | 0.102 | 0.080 | 0.062 | 0.011 | 0.057 | 0.919 |
| | 0.5 | 0.0 | 1.000 | 1.051 | 1.000 | 0.951 | 0.951 | 1.000 | 0.000 |
| | | 0.1 | 0.877 | 0.771 | 0.728 | 0.688 | 0.669 | 0.720 | 0.271 |
| | | 0.5 | 0.628 | 0.591 | 0.546 | 0.504 | 0.502 | 0.546 | 0.454 |
| | | 1.0 | 0.426 | 0.551 | 0.490 | 0.436 | 0.481 | 0.516 | 0.509 |
| 1.0 | -0.5 | 0.0 | 0.996 | 1.585 | 0.959 | 0.580 | 0.580 | 1.083 | 0.000 |
| | | 0.1 | 0.897 | 1.352 | 0.774 | 0.443 | 0.349 | 0.850 | 0.185 |
| | | 0.5 | 0.542 | 0.784 | 0.312 | 0.124 | -0.176 | 0.304 | 0.642 |
| | | 1.0 | 0.015 | 0.493 | 0.000 | 0.000 | -0.493 | 0.000 | 0.993 |
| | 0.0 | 0.0 | 0.996 | 1.585 | 0.959 | 0.580 | 0.580 | 1.083 | 0.000 |
| | | 0.1 | 0.909 | 1.416 | 0.817 | 0.471 | 0.424 | 0.920 | 0.142 |
| | | 0.5 | 0.598 | 1.014 | 0.440 | 0.191 | 0.104 | 0.559 | 0.507 |
| | | 1.0 | 0.215 | 0.824 | 0.081 | 0.008 | 0.001 | 0.413 | 0.824 |
| | 0.5 | 0.0 | 0.996 | 1.585 | 0.959 | 0.580 | 0.580 | 1.083 | 0.000 |
| | | 0.1 | 0.920 | 1.479 | 0.859 | 0.499 | 0.499 | 0.989 | 0.098 |
| | | 0.5 | 0.651 | 1.237 | 0.574 | 0.266 | 0.368 | 0.802 | 0.368 |
| | | 1.0 | 0.341 | 1.134 | 0.262 | 0.061 | 0.388 | 0.761 | 0.634 |
| 2.5 | -0.5 | 0.0 | 0.974 | 2.780 | 0.770 | 0.214 | 0.214 | 1.497 | 0.000 |
| | | 0.1 | 0.889 | 2.618 | 0.642 | 0.157 | 0.091 | 1.354 | 0.125 |
| | | 0.5 | 0.548 | 2.159 | 0.221 | 0.023 | -0.227 | 0.966 | 0.532 |
| | | 1.0 | 0.017 | 1.966 | 0.000 | 0.000 | -0.491 | 0.737 | 0.986 |
| | 0.0 | 0.0 | 0.974 | 2.780 | 0.770 | 0.214 | 0.214 | 1.497 | 0.000 |
| | | 0.1 | 0.894 | 2.661 | 0.657 | 0.106 | 0.146 | 1.404 | 0.106 |
| | | 0.5 | 0.571 | 2.349 | 0.264 | 0.030 | 0.016 | 1.182 | 0.470 |
| | | 1.0 | 0.023 | 2.443 | 0.000 | 0.000 | 0.000 | 1.221 | 0.977 |
| | 0.5 | 0.0 | 0.974 | 2.780 | 0.770 | 0.214 | 0.214 | 1.497 | 0.000 |
| | | 0.1 | 0.899 | 2.704 | 0.673 | 0.168 | 0.201 | 1.452 | 0.088 |
| | | 0.5 | 0.595 | 2.533 | 0.310 | 0.038 | 0.249 | 1.391 | 0.407 |
| | | 1.0 | 0.033 | 2.905 | 0.000 | 0.000 | 0.484 | 1.695 | 0.962 |
| 5.0 | -0.5 | 0.0 | 0.919 | 5.466 | 0.360 | 0.024 | 0.024 | 2.745 | 0.000 |
| | | 0.1 | 0.832 | 5.324 | 0.264 | 0.013 | -0.042 | 2.641 | 0.116 |
| | | 0.5 | 0.474 | 4.875 | 0.025 | 0.000 | -0.257 | 2.309 | 0.538 |
| | | 1.0 | 0.018 | 4.418 | 0.000 | 0.000 | -0.491 | 1.964 | 0.984 |
| | 0.0 | 0.0 | 0.919 | 5.466 | 0.360 | 0.024 | 0.024 | 2.745 | 0.000 |
| | | 0.1 | 0.834 | 5.366 | 0.268 | 0.013 | 0.012 | 2.689 | 0.107 |
| | | 0.5 | 0.482 | 5.089 | 0.029 | 0.000 | 0.000 | 2.545 | 0.509 |
| | | 1.0 | 0.021 | 4.899 | 0.000 | 0.000 | 0.000 | 2.500 | 0.980 |
| | 0.5 | 0.0 | 0.919 | 5.466 | 0.360 | 0.024 | 0.024 | 2.745 | 0.000 |
| | | 0.1 | 0.836 | 5.408 | 0.272 | 0.014 | 0.066 | 2.737 | 0.098 |
| | | 0.5 | 0.491 | 5.299 | 0.032 | 0.000 | 0.252 | 2.776 | 0.480 |
| | | 1.0 | 0.023 | 5.378 | 0.000 | 0.000 | 0.489 | 2.934 | 0.976 |

TABLE 1. Steady state values.

*TECHNICAL INFORMATION DEPARTMENT*
*LAWRENCE BERKELEY LABORATORY*
*UNIVERSITY OF CALIFORNIA*
*BERKELEY, CALIFORNIA 94720*